Relationship between the Fano asymmetry parameter and time-domain spectra studied by time-resolved measurement of carriers and phonons in *p*-type Si

Keiko Kato,[1,*] Yuya Hasegawa,[1,2] Katsuya Oguri,[1] Takehiko Tawara,[1] Tadashi Nishikawa,[2] and Hideki Gotoh[1]
[1]*NTT Basic Research Laboratories, 3-1 Wakamiya, Morinosato, Atsugi-shi, Kanagawa, 243-0198, Japan*
[2]*Tokyo Denki University, Department of Electronic Engineering, 5 Senju-Asahi-cho, Adachi-ku, Tokyo, 120-8551, Japan*

(Received 8 January 2018; published 2 March 2018)

We performed time-resolved reflectivity measurements in *p*-type Si to study the Fano asymmetry parameter as a function of time-domain parameters. We observed a fast decay of intervalence band transitions, and slow decay of optical phonons, which respectively correspond to the continuum and discrete states. The experimental results revealed that the initial phase of the discrete state and the ratio of the relative transition amplitude between the discrete and continuum states affect the Fano asymmetry parameter. We derived an equation for the Fano asymmetry parameter as a function of the time-domain parameters that explained the experimental results. The present study indicates how the Fano asymmetry parameter is controlled by the time-domain parameters.

DOI: 10.1103/PhysRevB.97.104301

I. INTRODUCTION

Quantum coupling between a discrete state and continuum states leads to an asymmetric line shape, known as a Fano resonance [1]. The number of publications devoted to Fano resonance is enormous because this phenomenon is observed in a variety of situations such as in photoabsorption in atoms [1], phonon spectra in solids [2], scanning tunneling microscopy [3], and plasmonic nanostructure [4]. Fano resonance has been investigated with frequency-domain spectroscopy, in which the spectrum is parametrized with the following equation:

$$I(\varepsilon) = \frac{(q+\varepsilon)^2}{1+\varepsilon^2}, \tag{1a}$$

$$\varepsilon = \frac{\omega - \Omega}{\Gamma/2}, \tag{1b}$$

where Ω and $\Gamma/2$ correspond to the resonance energy and dephasing rate of the discrete state, respectively, and q is the Fano asymmetry parameter that is used to characterize and quantify the asymmetric line shape. q is given by

$$q = \frac{\mathrm{V}\cdot(A_{\mathrm{dis}}/A_{\mathrm{con}}) + V^2 R(\varepsilon)}{\pi V^2 \rho(\varepsilon)}, \tag{2}$$

where A_{dis} and A_{con} correspond to the transition amplitude to the discrete and continuum states, respectively, V is the coupling constant between the discrete and continuum states, $\rho(\varepsilon)$ is the density of the continuum states, and $\pi^{-1}R(\varepsilon)$ is its Hilbert transform. As shown in Eq. (2), the Fano profile in the frequency-domain spectrum is sensitive to coupling between two states, which allows us to study the details of the interference process.

As an alternative method to conventional frequency-domain spectroscopies, time-resolved measurements have been used to study the dynamics of Fano resonance since the advent of ultrashort laser pulses [5–9]. The time-domain response of the Fano resonance is expressed as a sum of the discrete and continuum states [6,9],

$$I(t) = [A_{\mathrm{con}}\cdot\delta(t) + A_{\mathrm{dis}}\cdot e^{-(\Gamma/2)t}e^{i\phi}]e^{-i\Omega t}\cdot H_0(t), \tag{3}$$

where the first and second terms originate from the continuum states and discrete state, respectively. Here, ϕ corresponds to the phase of the discrete state with respect to the response of the continuum state, and $H_0(t)$ is the Heaviside step function. ϕ is observable by using time-domain techniques, whereas it cannot be observed by using frequency-domain techniques. In fact, optical control of q has been attempted by changing ϕ through the use of attosecond pulses [6]. While the dependence of q on ϕ [5,6,10] has been studied, its dependence on other time-domain parameters remains unknown. For further understanding of q in the time domain and for full control of q with ultrashort laser pulses, the relationship between q and all of the time-domain parameters must be understood. However, the time resolution has to be high enough to obtain all of the time-domain parameters, and an appropriate physical model is required to identify the signal relating to the Fano resonance. As far as we know, no study has been conducted that meets the above requirements, and we still do not know how all of the time-domain parameters relate to q.

In this study, we measured the time-resolved reflectivity of *p*-type Si to study the relationship between q and the time-domain parameters. In *p*-type Si, Fano resonance occurs through simultaneous excitation of the intervalence band transitions (IVT) and optical phonons (OP) [2,11]. IVT occur from the light-hole to heavy-hole bands when the Fermi level is lowered from the top of the valence band by *p*-type doping [Fig. 1(a)]. They occur in a certain region of k space and produce a broad continuum spectrum as shown in Fig. 1(b) [12]. The continuum spectrum overlaps with the discrete energy of OP, which results in the Fano-type asymmetric line shape in the Raman spectrum. By making time-resolved reflectivity measurements in *p*-type Si, we succeeded in identifying the time-domain parameters of IVT and OP [13,14]. Because

*kato.keiko@lab.ntt.co.jp

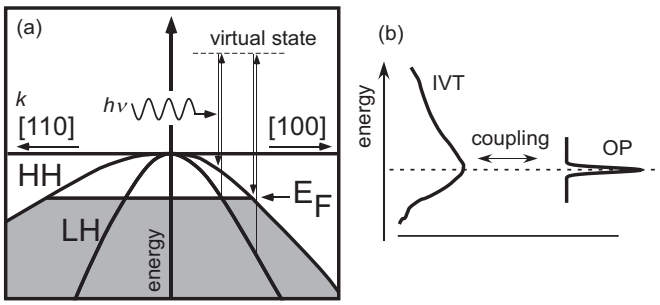

FIG. 1. (a) Energy diagram of the intervalence band transition in p-type Si. The vertical arrows show the intervalence band transitions from the light-hole to heavy-hole bands. E_F, HH, and LH correspond to the Fermi level, heavy-hole band, and light-hole band, respectively. (b) Schematic diagram of the Fano resonance in p-type Si. IVT and OP stand for the intervalence band transition and optical phonon, respectively.

q of p-type Si depends on temperature [2], the ultrafast dynamics should also exhibit a temperature dependence. Thus, we observed the time-domain spectrum of p-type Si while changing the temperature to clarify how the time-domain parameters relate to q.

II. EXPERIMENTAL

The time-resolved reflectivity measurements were performed to track the ultrafast dynamics of Fano resonance in p-type Si. To obtain IVT and OP signals with a good noise-to-signal ratio, we measured the anisotropic reflectivity, which eliminates the isotropic reflectivity change originating from the interband transition from the valence to conduction bands not relating to the Fano resonance [13,15]. The anisotropic reflectivity change ($\Delta R_{\mathrm{aniso}}$) was measured on Si(001) in the $\Gamma_{25'}$ geometry [8], and the polarizations of the pump and probe were parallel to [110] and [100], respectively. The light source was a mode-locked Ti:sapphire laser. The laser pulse duration was less than 10 fs, and the wavelength was centered at 780 nm. The pump power was $2.9(1) \times 10^{10}\,\mathrm{W/cm^2}$. The corresponding excited carrier density was estimated to be $8.0(1) \times 10^{17}/\mathrm{cm^3}$. The samples were nondoped and p-type Si. The carrier concentration in the p-type Si was more than $0.9(6) \times 10^{20}/\mathrm{cm^3}$, which is high enough to exhibit a Fano-type spectrum in a time-integrated Raman measurement [2]. To control q, we varied the temperature from 10 to 270 K

III. RESULTS AND DISCUSSION

The time-resolved anisotropic reflectivity of the p-type and nondoped Si taken at 10 K are shown as black lines in Figs. 2(a) and 2(b), respectively. Both samples exhibit a sharp response at $t = 0$ and an oscillatory signal with a repetition period of approximately 64 fs, which corresponds to the oscillation of OP in Si. On the one hand, the anisotropic reflectivity change in p-type Si can be decomposed into three components due to (1) the polarization grating (PG), (2) IVT, and (3) OP, in accordance with previous time-resolved measurements in

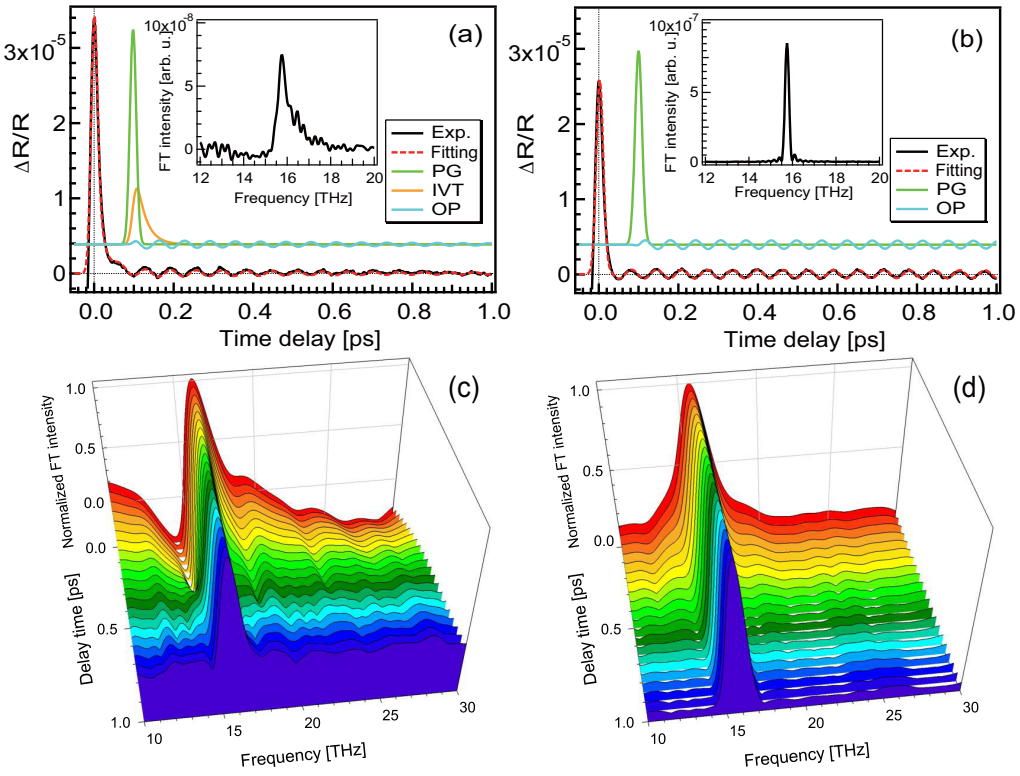

FIG. 2. Time-resolved anisotropic reflectivity of (a) p-type Si and (b) nondoped Si. Black and red lines are experimental and fitting results. Green, orange, and light-blue lines are components of the polarization grating, intervalence band transition, and optical phonons, respectively. The insets show the FT power spectra. Each component is shown with an offset. The CWT spectra of (c) p-type Si and (d) nondoped Si. The window function is a Gaussian with 400-fs full width at half maximum. The intensity is normalized.

Si [13,15]. On the other hand, the change in nondoped Si can be decomposed into PG and OP because IVT is observable under the condition that the Fermi level is lower than the top of the valence band (i.e., in p-type Si). IVT and OP, respectively, correspond to the excitation to the continuum and discrete state whereas PG originates from an overlap between the pump and probe pulses [15] and is not related to the Fano resonance. Each component can be expressed as follows:

$$\mathrm{PG}: f_{\mathrm{PG}} = A_{\mathrm{PG}} \cdot \exp\left(-\frac{\Delta t^2}{\tau_p^2}\right), \tag{4a}$$

$$\mathrm{IVT}: f_{\mathrm{IVT}} = A_{\mathrm{con}} \cdot \exp\left(-\frac{\Delta t}{\tau_{\mathrm{IVT}}}\right) \cdot \left[\mathrm{erf}\left(\frac{\Delta t}{\tau_p} - \frac{\tau_p}{2\tau_{\mathrm{IVT}}}\right) + 1\right] \Big/ 2, \tag{4b}$$

$$\mathrm{OP}: f_{\mathrm{OP}} = A_{\mathrm{dis}} \cdot \exp\left(-\frac{\Gamma}{2}\Delta t\right) \cos\{2\pi \nu_{\mathrm{OP}} \Delta t - \varphi\} \cdot \left[\mathrm{erf}\left(\frac{\Delta t}{\tau_p}\right) + 1\right] \Big/ 2, \tag{4c}$$

where A_{PG}, A_{con}, and A_{dis} correspond to the amplitudes of the polarization grating, intervalence band transition, and optical phonon, and Δt, τ_p, τ_{IVT}, $\Gamma/2$, ν_{OP}, and φ correspond, respectively, to the delay time, pulse width, decay time of IVT, phonon dephasing rate, phonon frequency, and initial phase. In fact, the experimental result (black line in Fig. 2) can be fitted to the sum of these components, as shown by the red dotted lines in Figs. 2(a) and 2(b). Thus, we succeeded in separately observing the dynamics of the discrete and continuum states in the Fano resonance.

Fourier transform (FT) analysis must be used to evaluate q from the time-domain signal. Before the FT analysis, it is important to extract the signals related to the Fano resonance from the whole of the signals because unrelated signals make it difficult to evaluate q correctly. Therefore, we subtracted the PG component and performed a FT on the remainder of the signal. We thereby obtained the power spectrum $I(\omega) = |\int_{-\infty}^{\infty} f(t)e^{-i\omega t}dt|^2$ to make a correspondence with the frequency-domain spectrum (i.e., the Raman spectrum), which is equivalent to the radiation spectrum of the dipole given by $|\int_{-\infty}^{\infty} d(t)e^{-i\omega t}dt|^2$, where $d(t)$ is a time-dependent dipole response [16]. The power spectrum is asymmetric in p-type Si but symmetric in nondoped Si, as shown in the insets in Figs. 2(a) and 2(b). Moreover, the origin of the asymmetric line shape in p-type Si could be clearly identified in the continuous wavelet transformation (CWT) spectra [17], which is useful for revealing the dynamical interference of coupled systems [8,18]. In Fig. 2(c), the CWT spectra of p-type Si change from asymmetric to symmetric as the delay elapses. The transient appearance of the Fano asymmetric profiles just after the pump excitation reflects the short lifetime of IVT, which is estimated to be 20 fs from the fitting. These results indicate that simultaneous excitations to the continuum and discrete states (i.e., IVT and OP) cause the Fano profile in the CWT spectra. In contrast, the CWT spectra of the nondoped Si appear symmetric at all delay times because of the absence of IVT (i.e., the excitation to the continuum state) as shown in Fig. 2(d).

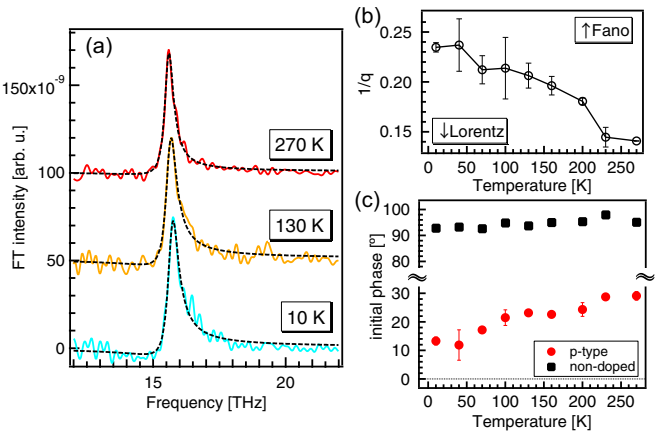

FIG. 3. (a) Temperature dependence of the FT spectra of p-type Si. (b) Temperature dependence of q. (c) Temperature dependence of the initial phase of p-type Si (red circles) and nondoped Si (black squares). The initial phase of the optical phonon (φ) is defined with respect to zero delay time.

The contrasting spectra between p-type and nondoped Si confirm that the signals relating to the Fano resonance could be extracted appropriately.

Next, we show the temperature dependence of the time-domain signals and q. The temperature dependence of the power spectrum is shown in Fig. 3(a). Here, we will focus our discussion on p-type Si because nondoped Si keeps a symmetric line shape at all temperatures. As the temperature decreases, the power spectrum of the p-type Si becomes more asymmetric. This behavior can be seen in the temperature dependence of q in Fig. 3(b). Next, let us see how the time-domain parameters (i.e., A_{con}, A_{dis}, τ_{IVT}, Γ, ν_{OP}, and φ) depend on the temperature. In Table I, τ_{IVT}, ν_{OP}, and φ exhibit temperature dependences. As the temperature decreases, τ_{IVT} and ν_{OP} increases and φ decreases. We thus have identified which time-domain parameters exhibit a temperature dependence and could be responsible for the temperature dependence of q.

Here, we briefly discuss the origin of the temperature dependence of the three parameters. The increase in τ_{IVT} would be due to less scattering from thermal carriers and/or phonons as the temperature decreases. As to the origin of the temperature dependence of ν_{OP}, the anharmonic decay and thermal expansion should be considered. The present result can be fitted only with an anharmonic decay [14,19]. In fact, a previous theoretical study showed that the anharmonic decay is dominant below 270 K [20]. φ shows a temperature dependence only in p-type Si, as shown in Fig. 3(c). The initial

TABLE I. Fitting parameters obtained at 270, 200, 100, and 10 K. The initial phase of the phonon (φ) is defined with respect to the zero delay time ($\Delta t = 0$).

	$A_{\mathrm{dis}}/A_{\mathrm{con}}$	τ_{IVT} (fs)	$\Gamma/2(\mathrm{ps}^{-1})$	ν_{OP} (THz)	φ (degree)
270 K	$3.7(3) \times 10^{-2}$	18.6(2)	1.4(2)	15.58(1)	29(2)
200 K	$4.3(2) \times 10^{-2}$	22.6(1)	1.37(4)	15.66(3)	24(3)
100 K	$4.0(5) \times 10^{-2}$	23.7(4)	1.4(1)	15.69(2)	21(3)
10 K	$4.0(3) \times 10^{-2}$	23.3(6)	1.40(1)	15.72(1)	13(2)

phase of the phonon in the p-type Si approaches the cosine phase as the temperature decreases, while that in the nondoped Si remains in the sine phase. This result should be noted because the initial phase usually reflects the phonon generation mechanism. In previous studies [21,22], phonons exhibited cosine oscillations in cases with the real electronic transitions (e.g., opaque materials), whereas they exhibited sine oscillations in cases without real electronic transitions (e.g., transparent materials). In accordance with the above picture, the nearly cosine phase observed in the p-type Si suggests that real transitions are dominant in the phonon generation while the sine phase observed in the nondoped Si suggests virtual transitions are dominant in the phonon generation. In fact, IVT occurs in p-type Si, and virtual transitions are considered to be the phonon generation mechanism in nondoped Si [21,23]. The temperature dependence of φ in the p-type Si suggests that the contribution of the IVT increases as the temperature decreases because φ approaches the cosine phase (i.e., 0°). Moreover, as the temperature decreases, the Fermi level is further lowered from the top of the valence band [24], which enables the real electronic transitions (i.e., IVT) to generate more phonons. Confirming the origin of the temperature dependence of φ, however, requires a detailed theoretical model for the phonon generation mechanism in p-type Si.

Then, we derive an equation for q as a function of time-domain parameters. On the one hand, the time-dependent response of the Fano resonance consists of the responses of the discrete and continuum states, as described by Eq. (3) [5,6,9]. In p-type Si, the first term corresponds to the response originating from IVT (i.e., f_{IVT}), whereas the second term corresponds to the response originating from OP (i.e., f_{OP}). On the other hand, the whole frequency-domain spectrum of the Fano resonance is given by

$$I_{\mathrm{total}}(\omega) = \sigma_a \frac{(q+\varepsilon)^2}{1+\varepsilon^2} + \sigma_b, \tag{5}$$

where σ_a and σ_b correspond to cross sections of transitions to the continuum states that do and do not interact with the discrete state [16]. Supposing that the power spectrum of Eq. (3) results in Eq. (5), we obtain the following equation for q as a function of the time-domain parameters:

$$q = \frac{-\mathrm{C} - \sqrt{\mathrm{C}^2+4}}{2}, \quad (0^\circ < \phi < 180^\circ), \tag{6a}$$

$$q = \frac{-\mathrm{C} + \sqrt{\mathrm{C}^2+4}}{2}, \quad (180^\circ < \phi < 360^\circ), \tag{6b}$$

$$C = \frac{2\cos\phi + \frac{A_{\mathrm{dis}}}{A_{\mathrm{con}}} \cdot \frac{2}{\Gamma} \cdot \frac{1}{\alpha}}{\sin\phi}. \tag{6c}$$

Here, we have assumed a time-domain response for a continuum state of the form $\exp(-t/\alpha)$, which is used in the analysis of time-domain signals in p-type Si [i.e., Eq. 4(b)].

Figure 4 plots q as a function of ϕ. This calculation used experimental values of $\Gamma/2$, and α are fixed, that is, 1.4 ps^{-1} and 23 fs. In this figure, the calculated results match the experimental results. Thus, it can be concluded that the temperature dependence of q in p-type Si is due to the phase shift of the discrete state. The observed monotonic behavior of q on ϕ appears when the second term in Eq. 6(c) is

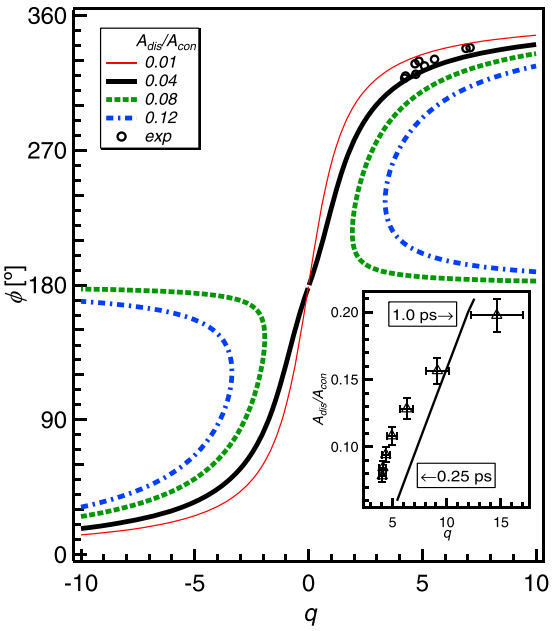

FIG. 4. Plot of q as a function of ϕ. ϕ is defined with respect to the response of the continuum states. Open circles are experimental results obtained at different temperatures. Thin, thick, dotted, and dashed lines were calculated using Eq. (6) for $A_{\mathrm{dis}}/A_{\mathrm{con}} =$ 0.01,0.04,0.08, and 0.12, respectively. The inset shows the dependence of q on $A_{\mathrm{dis}}/A_{\mathrm{con}}$. Triangles are q evaluated from the CWT spectra from 0.25 to 1.0 ps at 10 K. Solid line was calculated using Eq. (6) at $\phi = 320^\circ$.

small compared to the first term. Under such condition, q can be approximated as $-\cot(\phi/2)$, the same as in the previous time-resolved experiments [5,6,10]. However, when the second term cannot be ignored, the other time-domain parameters affect q as well. For example, the effect of $A_{\mathrm{dis}}/A_{\mathrm{con}}$ on q can be seen in the CWT spectra. In Fig. 2(c), the Fano profile in the p-type Si gradually disappears as the delay time passes; this is attributed to the decrease in $A_{\mathrm{dis}}/A_{\mathrm{con}}$. The inset of Fig. 4 plots $A_{\mathrm{dis}}/A_{\mathrm{con}}$ as a function of q. As the delay elapses from 0.25 to 1.0 ps, $A_{\mathrm{dis}}/A_{\mathrm{con}}$ increases and q increases in turn, and the measured values show as the calculated results. The dependence of q on $A_{\mathrm{dis}}/A_{\mathrm{con}}$ and Γ is a necessary consequence of Eq. (2). The first term in the numerator of Eq. (2) (i.e., $V \cdot A_{\mathrm{dis}}/A_{\mathrm{con}}$) leads to the $A_{\mathrm{dis}}/A_{\mathrm{con}}$ dependence in Eq. (6). Moreover, the denominator in Eq. (2) [i.e., $\pi V^2 \rho(\varepsilon)$] relates to the linewidth [25], which results in the dependence on $\Gamma/2$ in Eq. (6). When the second term of Eq. (6c), originating only from the discrete state, becomes large, the one-to-one relation between q and ϕ is broken (e.g., $A_{\mathrm{dis}}/A_{\mathrm{con}} = 0.08,0.12$ in Fig. 4). The situation occurs when the system is far from the resonance. Then, q keeps away from the origin (i.e., the resonance). Such a situation could not be observed under our experimental conditions, and is beyond the scope of the present work. Equation (6) reveals that not only ϕ, but also $A_{\mathrm{dis}}/A_{\mathrm{con}}$, Γ, and α relate to q.

Finally, we suggest a way of controlling q optically through $A_{\mathrm{dis}}/A_{\mathrm{con}}$ by changing the excitation photon energy. According to the time-integrated Raman measurements [2], on the one hand, q in p-type Si increases as with the excitation photon

energy (E_{ex}) without line broadening. On the other hand, the theoretical calculation indicates that the initial phase of the phonon should keep the sine phase if the photon energy is lower than the direct band gap (3.4 eV) [23]. Consequently, $A_{\rm dis}/A_{\rm con}$ would increase with E_{ex} without the initial phase shift, and this would result in a change in q. The present results suggest various ways of optically controlling q.

IV. CONCLUSION

In summary, we investigated how the time-domain signals of the Fano resonance relate to the Fano asymmetry parameter (i.e., q). Through time-resolved reflectivity measurements on p-type Si, we observed the ultrafast dynamics of the continuum and discrete states and determined the time-domain parameters relating to the Fano resonance. A continuous FT analysis revealed the transient appearance of the asymmetric Fano-type line shape during the intervalence band transition. By changing q with the temperature, we found which time-domain parameters exhibit temperature dependence. The observed temperature dependence of q could be explained by the temperature-induced shift in ϕ. Moreover, we found that q also depends on $A_{\rm dis}/A_{\rm con}$, and Γ, as might be expected from Fano's theory. The present results are valid for all systems that exhibit Fano resonance.

ACKNOWLEDGMENT

This study was supported by JSPS KAKENHI Grant No. 16H02120.

[1] U. Fano, Phys. Rev. **124**, 1866 (1961).
[2] F. Cerdeira, T. A. Fjeldly, and M. Cardona, Phys. Rev. B **8**, 4734 (1973).
[3] W. Chen, V. Madhavan, T. Jamneala, M. F. Crommie, and N. S. Wingreen, Science **280**, 567 (1998).
[4] B. Luk'yanchuk, N. I. Zheludev, S. A. Maier, N. J. Halas, P. Nordlander, H. Giessen, and C. T. Chong, Nat. Mater. **9**, 707 (2010).
[5] O.V. Misochko and M. V. Lebedev, J. Exp. Theor. Phys. **4**, 651 (2015).
[6] C. Ott, A. Kaldun, P. Raith, K. Meyer, M. Laux, J. Evers, C. H. Keitel, C. H. Greene, and T. Pfeifer, Science **340**, 716 (2013).
[7] M. Wickenhauser, J. Burgdorfer, F. Krausz, and M. Drescher, Phys. Rev. Lett. **94**, 023002 (2005).
[8] M. Hase, M. Kitajima, A. M. Constantinescu, and H. Petek, Nature (London) **426**, 51 (2003).
[9] U. Siegner, M.-A. Mycek, S. Glutsch, and D. S. Chemla, Phys. Rev. Lett. **74**, 470 (1995).
[10] D. M. Riffe, Phy. Rev. B **84**, 064308 (2011).
[11] F. Cerdeira, T. A. Fjeldly, and M. Cardona, Solid State Comm. **13**, 325 (1973).
[12] K. Arya, M. A. Kanehisa, M. Joanne, K. P. Jain, and M. Balkanski, J. Phys. C **12**, 3843 (1979).
[13] K. Kato, A. Ishizawa, K. Oguri, K. Tateno, T. Tawara, H. Gotoh, M. Kitajima, and H. Nakano, Jpn. J. Appl. Phys. **48**, 100205 (2009).
[14] K. Kato, K. Oguri, H. Sanada, T. Tawara, T. Sogawa, and H. Gotoh, AIP Adv. **5**, 097152 (2015).
[15] A. J. Sabbah and D. M. Riffe, Phys. Rev. B **66**, 165217 (2002).
[16] U. Fano and J. W. Cooper, Phys. Rev. **137**, A1364 (1965).
[17] C. K. Chui, *An Introduction to Wavelets* (Academic, San Diego, 1992).
[18] S. Yoshino, G. Oohata, and K. Mizoguchi, Phys. Rev. Lett. **115**, 157402 (2015).
[19] J. Menendez and M. Cardona, Phys. Rev. B **29**, 2051 (1984).
[20] S. Narasimhan and D. Vanderbilt, Phys. Rev. B **43**, 4541 (1991).
[21] D. M. Riffe and A. J. Sabbah, Phys. Rev. B **76**, 085207 (2007).
[22] R. Merlin, Solid State Commun. **102**, 207 (1997).
[23] Y. Shinohara, K. Yabana, Y. Kawashita, J.-I. Iwata, T. Otobe, and G. F. Bertsch, Phys. Rev. B **82**, 155110 (2010).
[24] W. P. Dumke, J. Appl. Phys. **54**, 3200 (1983).
[25] M. Chandrasekhar, H. R. Chandrasekhar, M. Grimsditch, and M. Cardona, Phys. Rev. B **22**, 4825 (1980).